

Supporting Information

Investigation of Emission Behaviour of Perovskite Nanocrystals into TiO₂ Nano to Microsphere

Abha Jha^a, Hari Shankar^a and Prasenjit Kar^{a*}

^aDepartment of Chemistry, Indian Institute of Technology Roorkee, Haridwar, Uttarakhand-247667, India.

Corresponding Email: kar.prasen@gmail.com, prasenjit.kar@cy.iitr.ac.in.

Table Of Content

Figure S1. The PL emission spectra of PNC/m-TiO₂ with increment in loading amount of TiO₂ solution.

Figure S2. DRS of prepared anatase TiO₂ microsphere with a bandgap of 3.2 eV by using an integrated sphere.

Figure S3. DRS of prepared TiO₂ nanoparticle with a bandgap of 3.6 eV by using an integrated sphere.

Figure S4. FTIR spectra of PNC-Tm, PNC and PNC-Tn shows the presence of functional group corresponding to the ligands. Whereas, PNC-Tm and PNC-Tn, show additional stretching vibrational frequency at 604 cm⁻¹ correspond to Ti-O-Ti indicating the titanium network present around the perovskite nanocrystals.

Table S1 Details of IR peak corresponding to PNC-Tm, PNC and PNC-Tn shows the presence of functional group corresponding to ligands.

Figure S5. SEM images of PNC shows the cubic morphology of perovskite nanocrystals at a scale bar of 200 nm.

Figure S6. TEM images of PNC shows the cubic morphology of perovskite nanocrystals at a scale bar of 50 nm.

Figure S7. Magnified TEM images of (a) m-TiO₂ (b) PNC-Tm depicted the pores are densely interconnected as microcrystalline spheres at a scale bar of 200 nm.

Figure S8. Shows the EDX and composition table of PNC-Tm with 1:3 of Pb and Br of MAPbBr₃ in pores of TiO₂ microsphere indicating the capping ligand don't affect the stoichiometry ratio of MAPbBr₃.

Figure S9. SEM images of TiO₂ microsphere at a scale bar of 200 nm.

Figure S10. TEM images of TiO₂ microsphere at a scale bar of 200 nm.

Figure S11. AFM image of TiO₂ microspheres with a Root Mean Square (RMS) value of 66.79 nm over an area of 25 μm².

Figure S12. (a) and (b) Fluorescence image of TiO_2 microspheres encapsulated with MAPbBr_3 Perovskite shows microsphere are fluorescence. (c) images of PNC and PNC-Tm in day light and under 365 nm UV light.

Figure S13. Thermal stability test of PNC at different temperature.

Figure S14. Thermogravimetric Analysis (TGA) of encapsulated TiO_2 microspheres with perovskite nanocrystals (PNC-Tm) indicate the weight loss of 25.52% could be attributed to the decomposition of perovskite nanocrystal from the encapsulated TiO_2 microspheres. This also suggests the loading of 25.52% PNC into m- TiO_2 .

Figure S15. Shows the day stability test of PNC indicating the degradation of PNC with shifting of photoluminescence intensity towards higher wavelength due to the growth of larger size of nanocrystals.

Figure S16. Shows the PL spectra which corresponds to moisture stability test of PNC-Tm with 30 μl of water indicating the 8.2% of the PL performance of perovskite was reduced compare to original after 100min storage.

Figure S17. Shows the PL spectra which corresponds to moisture stability test of PNC with 30 μl of water indicating the 31% of the PL performance of perovskite was reduced compare to original after 100min storage.

Figure S18. Absorption spectra of PNC-Tn in the (a) presence of oxygen and (b) in nitrogen (inert) atmosphere.

Figure S19. Photoluminescence (PL) spectra of MAPbBr_3 perovskite nanocrystals (PNC) and TiO_2 microspheres after separating from TiO_2 microspheres encapsulated with perovskites nanocrystals (T-PNC).

Table S2. Calculation of lowest unoccupied molecular orbital (LUMO) and highest occupied molecular orbital (HOMO) value of PNC-Tm, PNC and PNC-Tn.

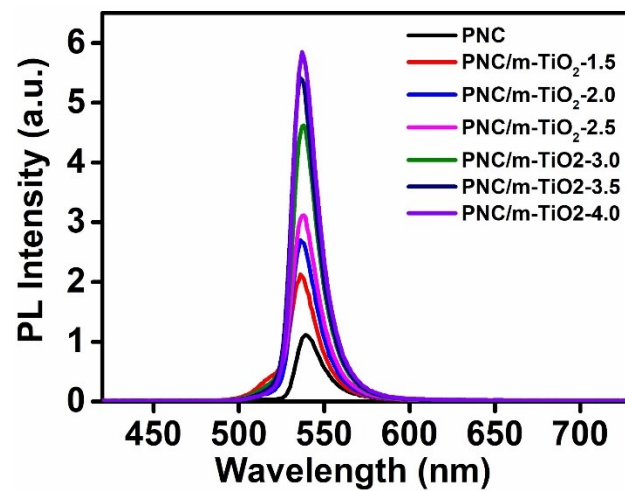


Figure S1. The PL emission spectra of PNC/m-TiO₂ with increment in loading amount of TiO₂ solution.

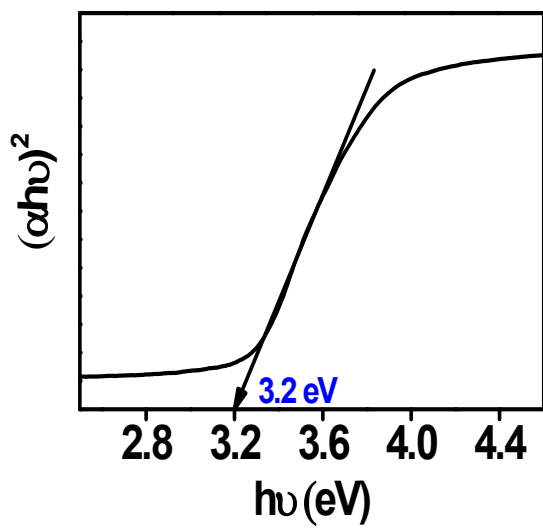


Figure S2. DRS of prepared TiO_2 microspheres with a bandgap of 3.2 eV by using an integrated sphere.

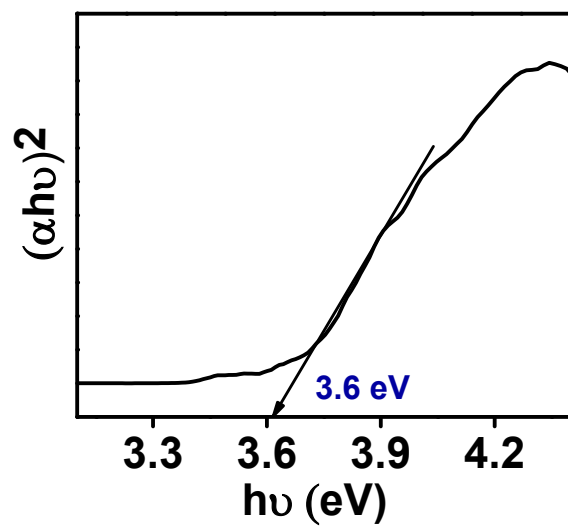


Figure S3. DRS of prepared TiO_2 nanoparticles with a bandgap of 3.6 eV by using an integrated sphere.

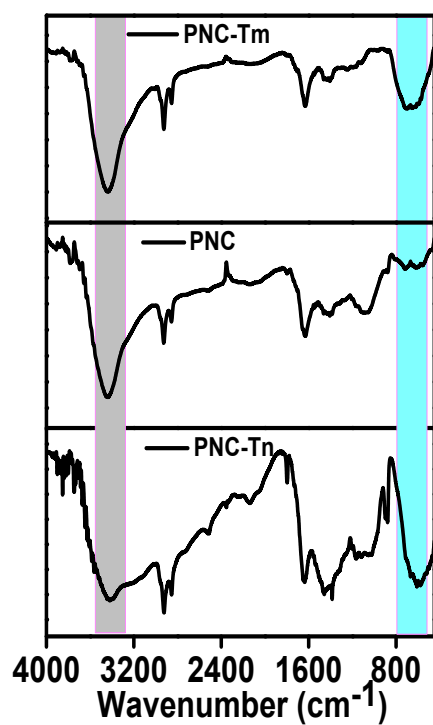


Figure S4. FTIR spectra of PNC-Tm, PNC and PNC-Tn shows the presence of functional group corresponding to the ligands. Whereas, PNC-Tm and PNC-Tn, show additional stretching vibrational frequency at 604 cm⁻¹ correspond to Ti-O-Ti indicating the titanium network present around the perovskite nanocrystals.

Table S1. Details of IR peak corresponding to PNC-Tm, PNC and PNC-Tn shows the presence of functional group corresponding to ligands.

S. No	Wavenumber (cm⁻¹)	Corresponding functional group
1	3441	Broad peak of -N-H stretching
2	2925	Symmetric stretching vibration of CH ₂
3	2856	Asymmetric stretching vibration of CH ₃
4	1631	COO ⁻ modes
5	1078	Out of plane bending mode of -CH
6	604	Asymmetric stretching vibrational frequency of Ti-O-Ti

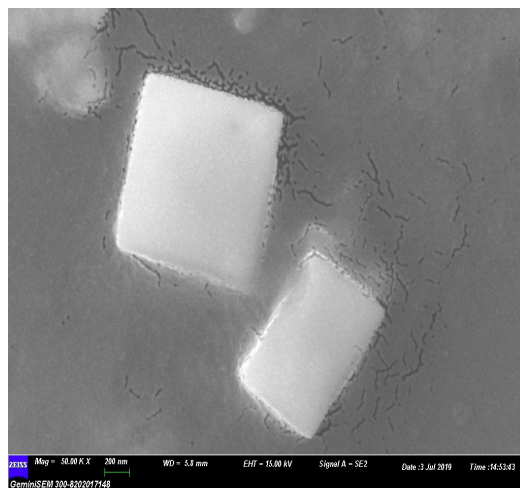


Figure S5. SEM images of PNC show the cubic morphology of perovskite nanocrystals at a scale bar of 200 nm.

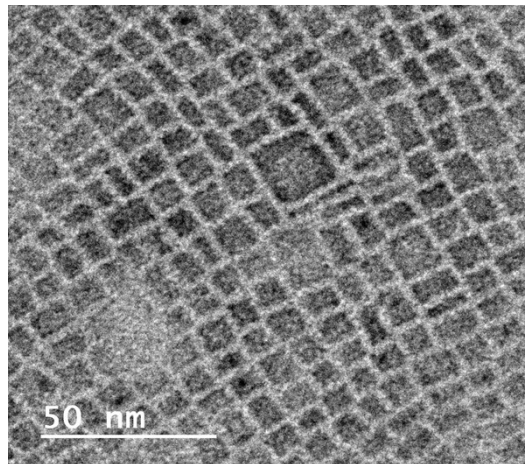


Figure S6. TEM images of PNC shows the cubic morphology of perovskite nanocrystals at a scale bar of 50 nm.

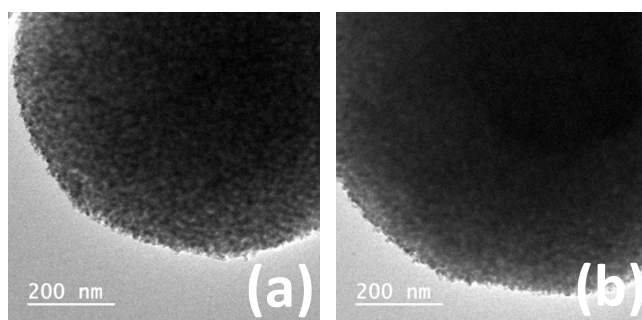


Figure S7. Magnified TEM images of (a) m-TiO₂ (b) PNC-Tm depicted the pores are densely interconnected as microcrystalline spheres at a scale bar of 200 nm.

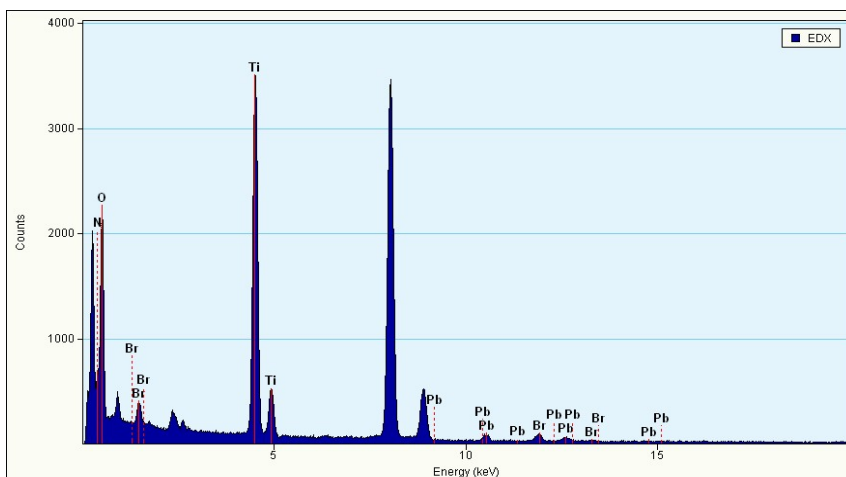


Figure S8. Shows the EDX and composition table of PNC-Tm with 1:3 of Pb and Br of MAPbBr₃ in pores of TiO₂ microspheres indicating the capping ligand don't affect the stoichiometry ratio of MAPbBr₃.

Element	Weight %	Atomic %	Uncert. %	Detector Correction	K-Factor
N (K)	9.82	19.87	0.27	0.28	3.466
O (K)	25.37	44.95	0.29	0.51	1.889
Ti (K)	55.38	32.78	0.32	0.98	1.227
Br (K)	5.04	1.79	0.11	0.99	2.575
Pb (L)	4.34	0.59	0.12	0.99	4.668

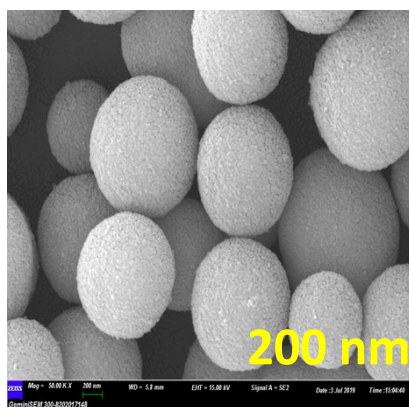


Figure S9. Shows the SEM images of TiO₂ microspheres at a scale bar of 200 nm.

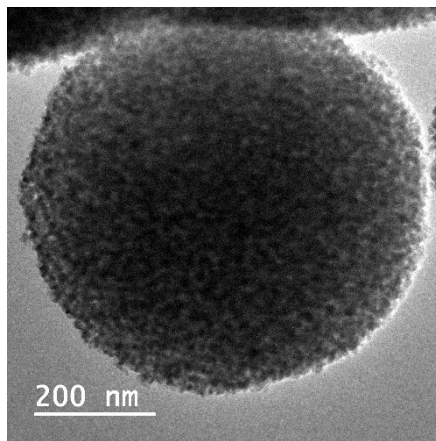


Figure S10. Shows the TEM images of TiO₂ microspheres at a scale bar of 200 nm.

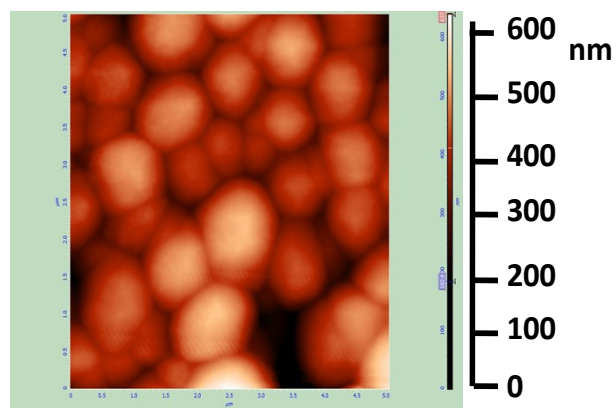


Figure S11. AFM image of TiO₂ microspheres with a Root Mean Square (RMS) value of 66.79 nm over an area of 25 μm².

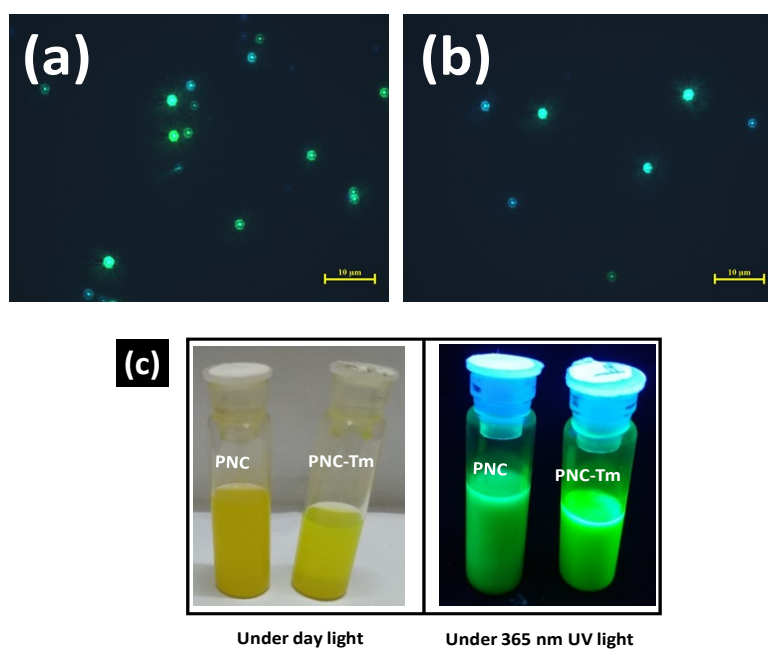


Figure S12. (a) and (b) Shows the fluorescent images of PNC-Tm at a scale bar of 10 μm indicating the TiO₂ microspheres is fluorescent after encapsulation with MAPbBr₃ perovskite. (c) images of PNC and PNC-Tm in day light and under 365 nm UV light.

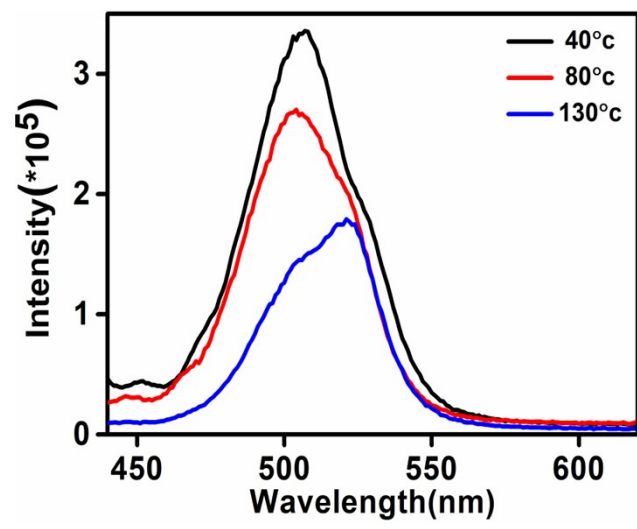


Figure S13. Thermal stability test of PNC at different temperature.

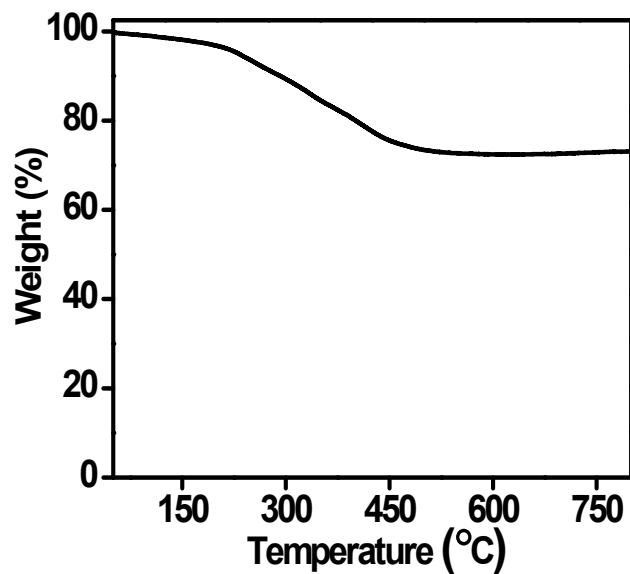


Figure S14. Thermogravimetric Analysis (TGA) of encapsulated TiO_2 microspheres with perovskite nanocrystals (PNC-Tm) indicate the weight loss of 25.52% could be attributed to the decomposition of perovskite nanocrystal from the encapsulated TiO_2 microspheres. This also suggests the loading of 25.52% PNC into m- TiO_2 .

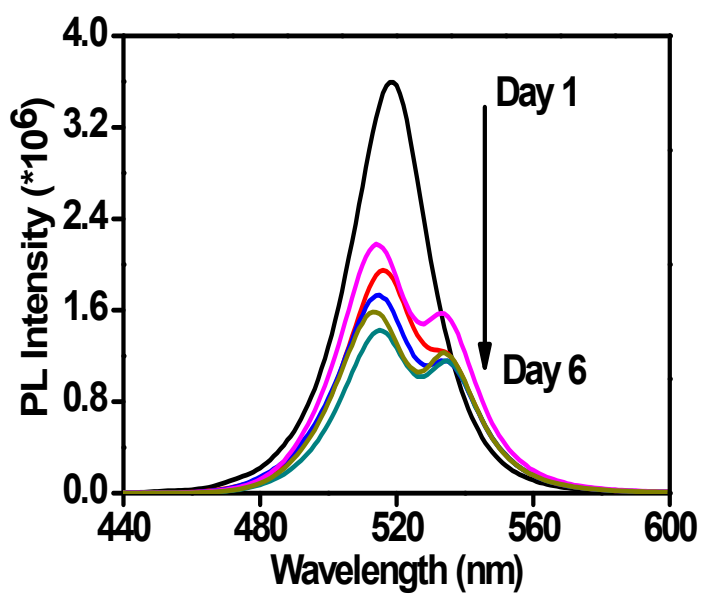


Figure S15. Shows the day stability test of PNC in solution form indicating the degradation of PNC with shifting of photoluminescence intensity towards higher wavelength due to the growth of larger size of nanocrystals.

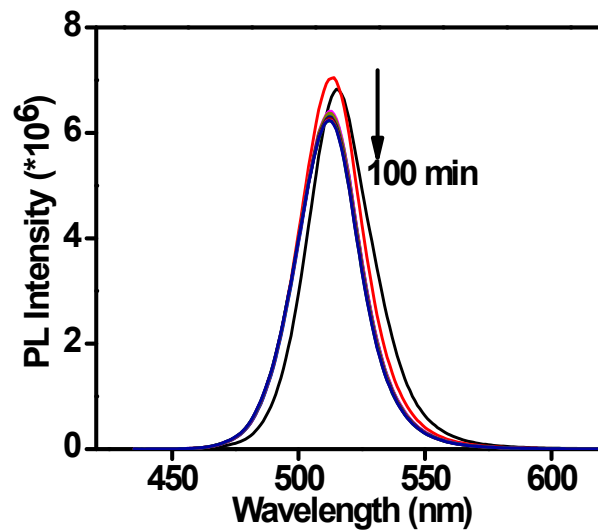


Figure S16. Shows the PL spectra which corresponds to moisture stability test of PNC-Tm with 30 μ l of water indicating the 8.2% of the PL performance of perovskite was reduced compare to original after 100min storage.

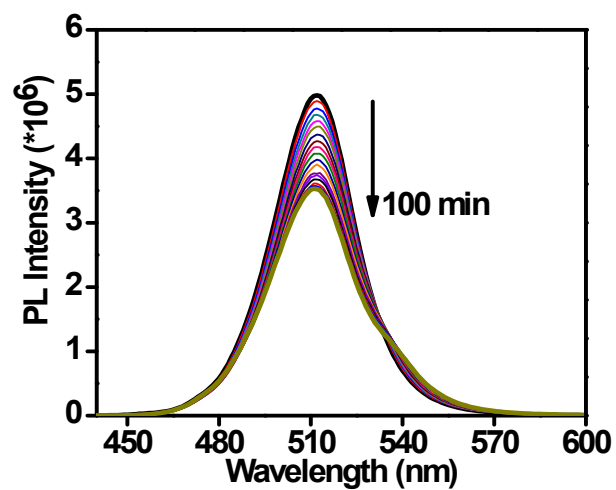


Figure S17. Shows the PL spectra which corresponds to moisture stability test of PNC with 30 μ l of water indicating the 31% of the PL performance of perovskite was reduced compare to original after 100min storage.

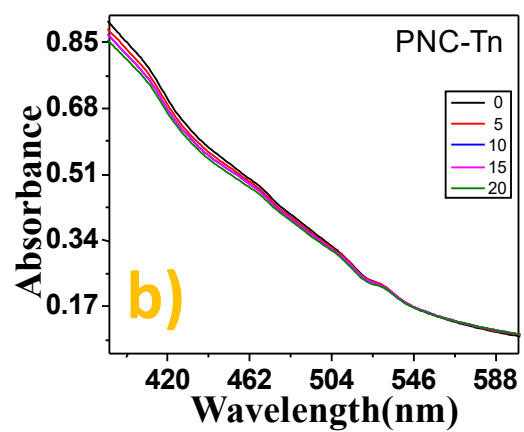
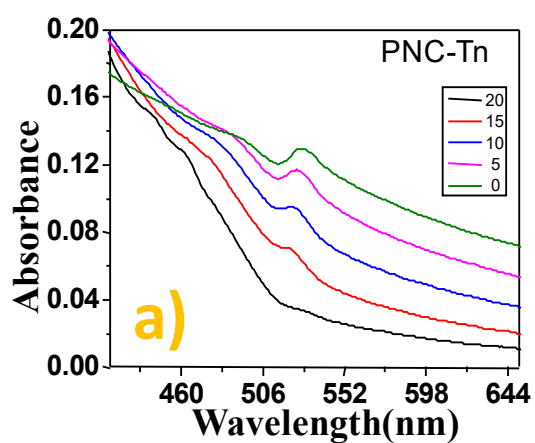


Figure S18. Absorption spectra of PNC-Tn in the (a) presence of oxygen and (b) in nitrogen (inert) atmosphere.

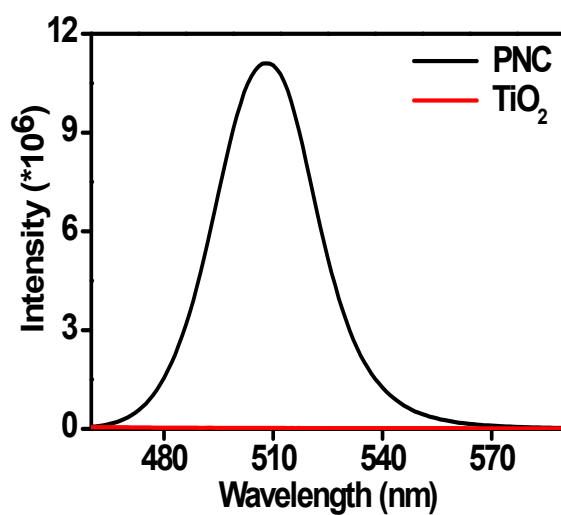


Figure S19. Photoluminescence (PL) spectra of MAPbBr₃ perovskite nanocrystals (PNC) and TiO₂ microspheres after separating from TiO₂ microspheres encapsulated with perovskites nanocrystals (T-PNC).

TiO₂ can be separated from the T-PNC at room temperature by sedimentation process and TiO₂ can be reusable after washing with ethanol followed by centrifugation. After that, PL spectra of TiO₂ has been taken, which shows the no fluorescence

PNC-Tm	PNC	PNC-Tn
$E_{\text{LUMO}} = -e (E_{\text{red}} + 4.4)$ $= - (-0.82 + 4.4)$ $= - 3.56 \text{ eV}$	$E_{\text{LUMO}} = -e (E_{\text{red}} + 4.4)$ $= - (-0.83 + 4.4)$ $= - 3.57 \text{ eV}$	$E_{\text{LUMO}} = -e (E_{\text{red}} + 4.4)$ $= - (-0.71 + 4.4)$ $= - 3.69 \text{ eV}$
$E_{\text{HOMO}} = E_{\text{LUMO}} - E_{\text{g}}$ $= -3.56 - 2.26$ $= -5.82 \text{ eV}$	$E_{\text{HOMO}} = E_{\text{LUMO}} - E_{\text{g}}$ $= -3.57 - 2.43$ $= -6.00 \text{ eV}$	$E_{\text{HOMO}} = E_{\text{LUMO}} - E_{\text{g}}$ $= -3.69 - 2.31$ $= -6.00 \text{ eV}$

Table S2. Calculation of lowest unoccupied molecular orbital (LUMO) and highest occupied molecular orbital (HOMO) value of PNC-Tm, PNC and PNC-Tn.